International Journal of Remote Sensing
Vol. 27, No. 18, 20 September 2006, 3881–3902

Taylor & Francis
Taylor & Francis Group

Predicting slow-drying fire weather index fuel moisture codes with NOAA-AVHRR images in Canada's northern boreal forests

STEVEN OLDFORD†, BRIGITTE LEBLON*†, DAVID MACLEAN† and MICHAEL FLANNIGAN‡

†Faculty of Forestry and Environmental Management, P.O. Box 44555, 28 Dineen Drive, University of New Brunswick, Fredericton, New Brunswick, Canada, E3B 6C2
‡Canadian Forest Service, Natural Resources Canada, 1219 Queen Street East, Sault Ste. Marie, Ontario, Canada, P6A 5M7

(*Received 25 September 2005; in final form 17 February 2006*)

Fire danger predicted by the Canadian Fire Weather Index, a system based on point-source weather records, is limited spatially. NOAA-AVHRR images were used to model two slow-drying fuel moisture codes, the duff moisture code and the drought code of the fire weather index, in boreal forests of a 250,000 km^2 portion of northern Alberta and the southern Northwest Territories, Canada. Temporal and spatial factors affecting both codes and spectral variables (normalized difference vegetation index, surface temperature, relative greenness, and the ratio between normalized difference vegetation index and surface temperature) were identified. Models were developed on a yearly and seasonal basis. They were strongest in spring, but had a tendency to saturate. Drought code was best modelled (R^2=0.34–0.75) in the spring of 1995 when data were categorized spatially by broad forest cover types. These models showed improved spatial resolution by mapping drought code at the pixel level compared to broadly interpolated weather station-based estimates. Limitations and possible improvements of the study are also discussed.

1. Introduction

Forests cover nearly 42% of Canada's land area, over half of which produce merchantable timer. About 9000 forest fires occur yearly in Canada, burning more than two million hectares and incurring nearly half a billion dollars in suppression costs (Canadian Council of Forest Ministers 2004). In Canada, fire danger is rated daily using the Canadian Forest Fire Danger Rating System (CFFDRS), a semi-empirical modular system that utilizes weather, fuel, topography, and ignition parameters as inputs through four subsystems (Stocks *et al.* 1989). One of the subsystems, the Canadian Fire Weather Index (FWI) system, computes potential mid-afternoon fire danger from noon-time weather station records of dry bulb temperature, relative humidity, 10 m high open wind speed, and 24-hour precipitation measurements (Van Wagner 1987).

The FWI system is comprised of three moisture codes: the fine fuel moisture code (FFMC) represents quick-drying surface litter fine fuel moisture contents, the duff moisture code (DMC) represents slow-drying, moderate depth, loosely compact duff moisture contents, and the drought code (DC) represents slow-drying, deep layer,

*Corresponding author. Email: bleblon@unb.ca

International Journal of Remote Sensing
ISSN 0143-1161 print/ISSN 1366-5901 online © 2006 Taylor & Francis
http://www.tandf.co.uk/journals
DOI: 10.1080/01431160600784234

compact organic matter moisture contents. These three moisture codes have time lags of two-thirds of a day, 15 days, and 53 days, respectively (Lawson *et al.* 1997). Time lags represent the time necessary for a fuel type to lose about two-thirds of its free moisture at equilibrium (when air temperature is 20°C and relative humidity is 40%) (Van Wagner 1987). Derived from these three moisture codes and wind speed, two indices provide a measure of the initial fire spread rate, the initial spread index (ISI), and the total fuel available for combustion, the build-up index (BUI). The FWI is then calculated from the combination of ISI and BUI (Van Wagner 1987).

The FWI is a useful measure of general fire danger for administrative purposes over large geographic regions (Stocks *et al.* 1989). However, the FWI system does not consider environmental conditions at finer spatial scales since it uses point measurements from often widely dispersed weather stations. Fuel moisture measurements made at weather stations, from meteorological variables, are limited spatially because accuracy decreases as the distance between weather station increases.

Satellite remote sensing potentially can complement current fire danger measurements because it can map several CFFDRS parameters. These parameters are not only related to topography, plant phenology, and fuel type, but also to fuel moisture, which is an important FWI system parameter. In previous studies, fuel moisture has been estimated primarily from NOAA-AVHRR normalized difference vegetation index (NDVI) images alone, or in combination with absolute maximum and minimum NDVI (relative greenness) (e.g. Paltridge and Barber 1988, Lopez *et al.* 1991, Illera *et al.* 1996, Burgan *et al.* 1998, Chuvieco *et al.* 1999). Thermal-infrared NOAA-AVHRR images also have been used (e.g. Dominguez *et al.* 1994, Chuvieco *et al.* 1999) because surface temperatures (T_s) increase with drought (Pierce *et al.* 1990).

An unavoidable problem of using optical and thermal-infrared remotely sensed images, such as T_s and NDVI, is pixel contamination caused by clouds, directional and off-nadir viewing effects, atmospheric interferences, solar angle effects, and shadows. These effects can be minimized with the use of maximum value composite (MVC) imaging techniques (Holben 1986). MVC images most often are created by assigning to each pixel the maximum NDVI value for a particular pixel over a composite period. Image composites of other variables retrieved from different channels on the same satellite sensor, such as T_s, are created at the same acquisition time as the maximum NDVI. In previous studies using MVC images, composite periods varied from three days (Eidenshink *et al.* 1989) to ten days (Dominguez *et al.* 1994).

As reviewed by Leblon (2001, 2005) and Camia *et al.* (2003), most studies estimating live fuel moisture used NOAA-AVHRR composite images, but other studies have used these images for estimating dead fuel moisture as represented by FWI system components. NOAA-AVHRR composite NDVI and T_s data were best correlated to FWI codes representing slow-drying fuels (DMC, DC, and BUI) over boreal forests and grasslands in Saskatchewan and Manitoba (Dominguez *et al.* 1994), northern boreal forests of the Mackenzie River basin, Northwest Territories (Leblon *et al.* 2001), and Mediterranean forests of Andalucia, southern Spain (Aguado *et al.* 2003). Aguado *et al.* (2003) attributed the good relationship between slow-drying fuel moisture and spectral variables to the slow temporal change of both the fuel moisture code and the spectral variables (DC time lag of 53 days and 10-day MVC NOAA-AVHRR images).

Desbois and Vidal (1995) showed that over Mediterranean forests, fire ignition occurred primarily in the hot zones of NOAA-AVHRR T_s images acquired just before a fire ignition date. Oldford *et al.* (2003) followed the method of Desbois and Vidal (1995) and in 1994 found that over the northern boreal forests of the Northwest Territories, Canada, there was a positive trend in mean T_s as the day of fire ignition approached. Aguado *et al.* (2003) combined optical and thermal-infrared NOAA-AVHRR images and successfully used them to model and map DC in Mediterranean forests. Similar to the methods of Aguado *et al.* (2003), this study modelled and mapped DMC and DC from optical and thermal-infrared images, but in the northern boreal forests of Canada.

The objective of this study is to determine if NOAA-AVHRR optical and thermal-infrared remote sensing images are related to slow-drying dead fuel moisture conditions, as parameterized by DMC and DC of the FWI system, in northern boreal forests. We used data acquired between 1993 and 1999 over boreal forests in northern Alberta and southern Northwest Territories, Canada, and developed multiple regression models between DMC and DC as dependent variables, and spectral variables derived from 10-day composite NOAA-AVHRR NDVI and T_s images as independent variables. Due to the complex structural nature of boreal forests, canopies may not be fully closed. In this study, fuel moisture is assessed from spectrally derived variables and refers to a mixture of both live canopy fuel moisture and dead under-storey soil fuel moisture. By studying strictly boreal forests, this study differs from previous ones that studied European Mediterranean forests (e.g. Lopez *et al.* 1991, Illera *et al.* 1996, Camia *et al.* 1999, Chuvieco *et al.* 1999, Aguado *et al.* 2003) and boreal forest and grassland cover types over Western Canada (Dominguez *et al.* 1994).

2. Methods

2.1 *Study area*

Our study area was located in northern Alberta and the southern Northwest Territories, Canada, between 54° and 62° north latitude and 110° and 115° west longitude (figure 1). Covering approximately 250,000 km^2, it includes a variety of forested and non-forested land cover types (figure 2). It is primarily within the Boreal Plains Ecozone of Canada and includes portions of the Taiga Shield, Taiga Plain, and Prairie Ecozones (Rowe 1972).

2.2 *Materials*

We used weather station, satellite imagery, and cartographic data collected between 1993 and 1999 (table 1).

Weather data, including noon-time dry bulb temperature, relative humidity, and 24-hour precipitation, collected daily at 75 different weather stations within the study area (figure 2), were used to calculate DMC and DC components of the Canadian FWI system. 10 m high open wind speed, a fourth weather variable used in calculating the FWI, is not used in calculating DMC and DC. This variable is used in calculating the FFMC, a quick-drying fuel moisture code, and the ISI, a measure of potential initial fire spread rate.

A comparison between annual precipitation accumulation with respect to climatologic normals showed that during the studied period, there were two wet

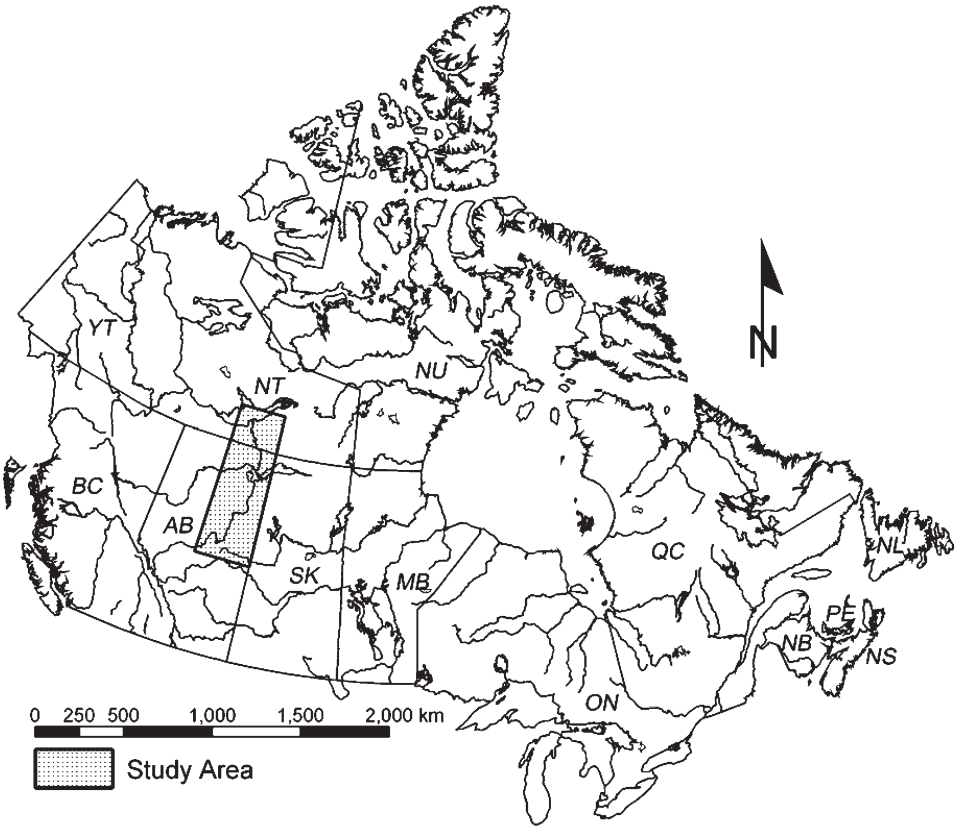

Figure 1. Study area location in Canada.

years (1996 and 1997), three normal years (1993, 1994, and 1995), and two dry years (1998 and 1999) (Oldford 2004).

Spectral data were used to model and map fuel moisture conditions within the study area. A total of 140 NOAA-AVHRR 10-day MVC images (20 images per year) were obtained between 11 April and 31 October. Images were acquired by the NOAA-11 satellite in 1993 and 1994 and the NOAA-14 satellite between 1995 and 1999. The 10-day compositing was carried out at the Manitoba Remote Sensing Center following the 'Geocoding and Compositing' (GEOCOMP) system developed by the Canada Center for Remote Sensing (CCRS). Through this method, images were georeferenced into a Lambert conformal conic projection. Each image had a spatial resolution of 1 km^2. Images were further processed with the Atmosphere, Bidirectional, and Contamination Corrections Software System version 2 (ABC3v2) (Cihlar *et al.* 1997a,b). This system applied refined radiometric calibration and other product enhancements so images were as free as possible from residual error such as the effects of not representing the surface under uniform illumination and viewing conditions.

T_s images were derived from the brightness temperature of NOAA-AVHRR channels four (10.3–11.3 μm) and five (11.5–12.5 μm), corrected for atmospheric and surface emissivity effects. NDVI images were derived from NOAA-AVHRR channels two (0.725–1.10 μm) and one (0.58–0.68 μm). NDVI images were corrected with a bidirectional reflectance function (BDRF) based on BDRF-corrected surface

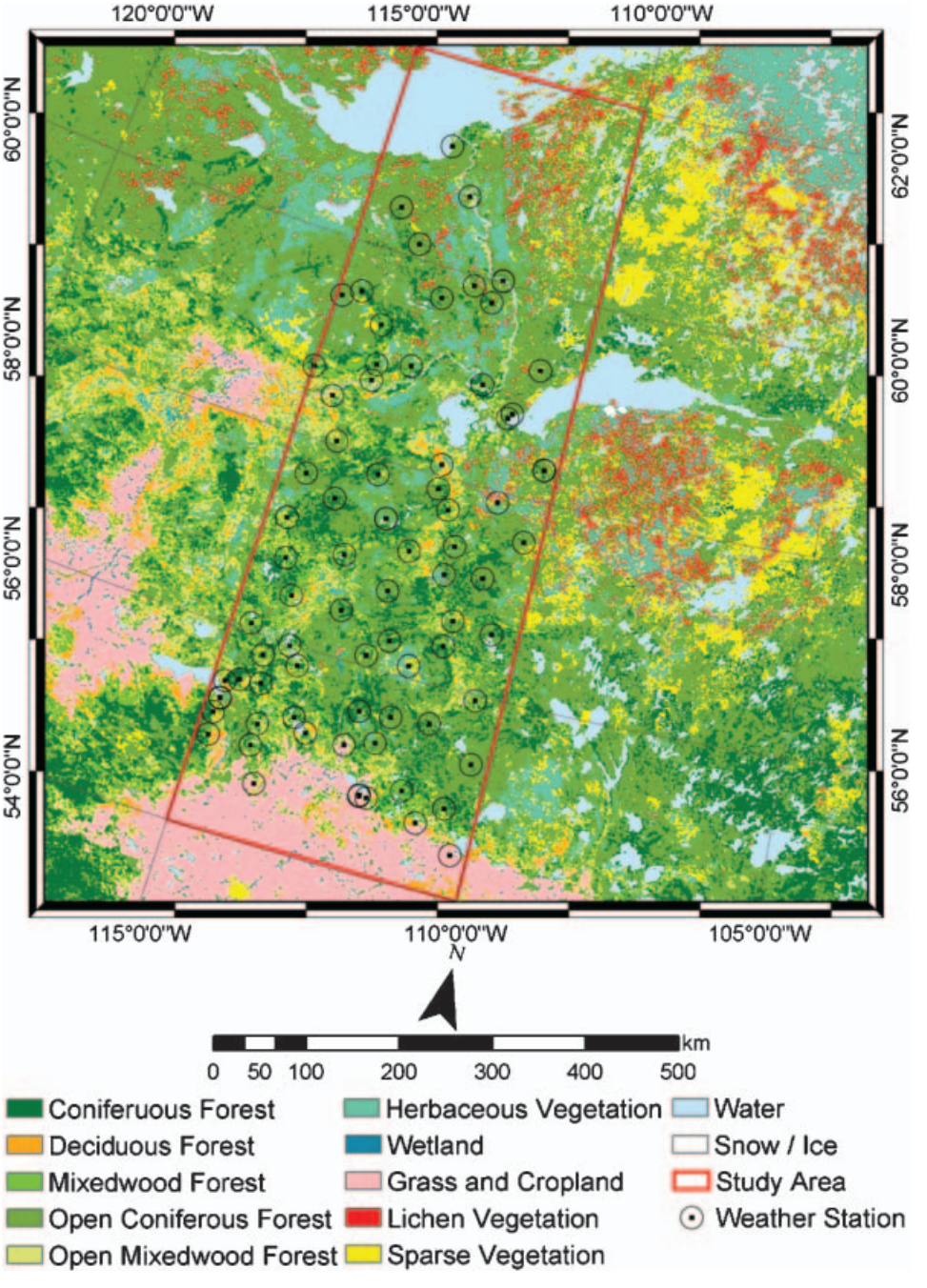

Figure 2. Weather station locations within the study area and land cover derived from the 1998 SPOT-4 VEGETATION 12-class land cover map of Canada (after Cihlar *et al.* 2002).

reflectance for NOAA-AVHRR channels one and two. The cloud elimination from composites using albedo and NDVI trend (CECANT) procedure, developed by Cihlar (1996), was used to identify contaminated pixels in T_s and NDVI images. The CECANT procedure identifies surface vegetation, bare soil, rock, or open water

Table 1. Spatial and temporal resolutions of spectral, weather and cartographic data used in this study.

Data type/ variable[1]	Year(s)	Resolution		Data source	
		Spatial[2]	Temporal	Source	Agency[3]
Spectral					
T_s	1993–1999	1 km^2	10 days	10-day MVC NOAA-AVHRR	CCRS
NDVI	1993–1999	1 km^2	10 days	10-day MVC NOAA-AVHRR	CCRS
Land cover	1998	1 km^2	1 year	SPOT-4 VEGETATION	CCRS
Weather					
DMC & DC	1993–1999	Point source	Daily	Weather stations	EC
DMC & DC	1993–1999	Point source	Daily	Weather stations	AB
DMC & DC	1993–1999	Point source	Daily	Weather stations	NT
DMC & DC	1993–1999	Point source	Daily	Weather stations	WB
Cartographic					
Elevation	1999	1 km^2	1 year	DEM of Canada	Geogratis

[1]DC, drought code; DMC, duff moisture code; NDVI, normalized difference vegetation index; T_s, surface temperature.
[2]Point source: spatial resolution is variable depending on the density of weather stations.
[3]AB, Alberta Department of Energy and Environment; CCRS, Canada Center for Remote Sensing; EC, Environment Canada; NT, Northwest Territories Forest Management Division; WB, Wood Buffalo National Park.

pixels that are obscured by clouds, partial clouds, cloud shadows, smoke, other heavy aerosols, snow, and ice. For those contaminated pixels, seasonal interpolation was used to correct NDVI and T_s images, provided that at least three uncontaminated composite period values were available within a year (Canada Center for Remote Sensing 2000). According to the Canada Center for Remote Sensing (2000), this dataset approximates nadir-viewed composite images obtained under cloud-free conditions during the growing season better than MVC alone. NDVI and T_s images were used to compute the ratio between NDVI and T_s, and relative greenness (RGRE). RGRE is derived from NDVI values and indicates how green a pixel is in relation to its historical range of NDVI values (Burgan *et al.* 1996).

Spectral data were retrieved only from forested pixels, identified in the 1998 Canada-wide land cover map made from SPOT-4 VEGETATION images (figure 2) (Cihlar *et al.* 2002).

Elevations of weather stations within the study area were determined from a digital elevation map of Canada, with a spatial resolution of 1 km^2 (Geogratis Canada 2000). Elevation was considered because topographic conditions can influence remote sensing data (Guindon *et al.* 1982, Teillet *et al.* 1982) and weather station measurements (Flohn 1969).

2.3 *Data analyses*

DMC and DC were calculated from weather station data by using a SAS (SAS Institute 2001) script provided by the Canadian Forest Service with latitude, longitude, year, month, day, temperature, relative humidity, and precipitation as inputs. Each DMC and DC record was assigned a time period corresponding to the 10-day period classification used in NOAA-AVHRR composite images. Medians

were calculated for each image period/station group because they were less affected than means by extreme observations that potentially resulted from data processing errors. Weather station medians were excluded from further analysis if any data were missing within a 10-day period. This resulted in 15% of periodic weather station data being excluded from further analysis.

A point location map of the 75 study area weather stations was overlaid on the study area land cover map (figure 2) and 3×3 pixel windows ($9\,km^2$) were identified in a block of continuous forested land nearest to each weather station. Forested land was defined as any of the four 'tree dominated' land types classified in the 1998 SPOT-4 VEGETATION land cover map of Canada (Cihlar *et al.* 2002) (figure 2). Forested land types included closed canopy coniferous, closed canopy mixedwood, open canopy coniferous, and open canopy mixedwood. A coniferous forest type is defined as having greater than 75% of the tree canopy composed of evergreen needle-leaf tree species. A mixedwood forest type is defined as having between 25 and 75% of the total tree cover composed of evergreen needle-leaf or deciduous broad-leaf tree species. Closed canopy conditions are defined as having greater than 60% crown cover, and open canopy conditions are defined as having between 25 and 60% crown cover (Cihlar *et al.* 2002). Pixel windows were identified on each NOAA-AVHRR image, and the values for NDVI, RGRE, T_s, and NDVI/T_s variables were extracted. Medians of nine pixel window values were calculated for each of the 140 images, 75 weather stations, and four spectral variables.

Both the DC and DMC median values and spectral values were used first in correlation analysis and then in a forward stepwise multiple regression analysis using the PROC REG procedure of SAS (SAS Institute 2001). A detailed description of study methodologies is given in Oldford (2004).

3. Results and discussion

3.1 *Temporal and spatial variability of FWI codes and spectral variables*

Both FWI codes and spectral variables exhibited temporal (figure 3) and spatial (figure 4) variability. Factors influencing temporal variability include year and season (as represented by the 10-day composite period), whereas those influencing spatial variability include elevation, latitude, and broad forest cover type at weather stations. An *F*-test analysis was conducted to determine the relative influence of these factors on FWI codes and spectral variables (table 2). Different satellite overpass times meant that spectral differences existed in data acquired from NOAA-11 and NOAA-14 years. Thus, separate ANOVA tests were performed for each satellite dataset.

For both satellite datasets, temporal factors and their interactions had the greatest influence on DC and DMC and on spectral variables. Generally, year had a greater influence on DC and DMC than the year's period, and the opposite was true for spectral variables, particularly for the NOAA-14 dataset. As a result, wet or dry years had a greater influence on DC and DMC than on spectral variables.

The influence of period was stronger for DC than DMC because DC showed an increasing trend throughout the growing season (figure 3(*a*)), while DMC was more variable (figure 3(*b*)). NDVI, RGRE, and T_s followed clear seasonal trends and were influenced less by yearly variations (figure 3(*c*), (*d*), (*e*)).

As expected, different forest cover type had a noticeable influence on NDVI. In all years, mean open coniferous NDVI values were 10%, 15%, and 11% less than

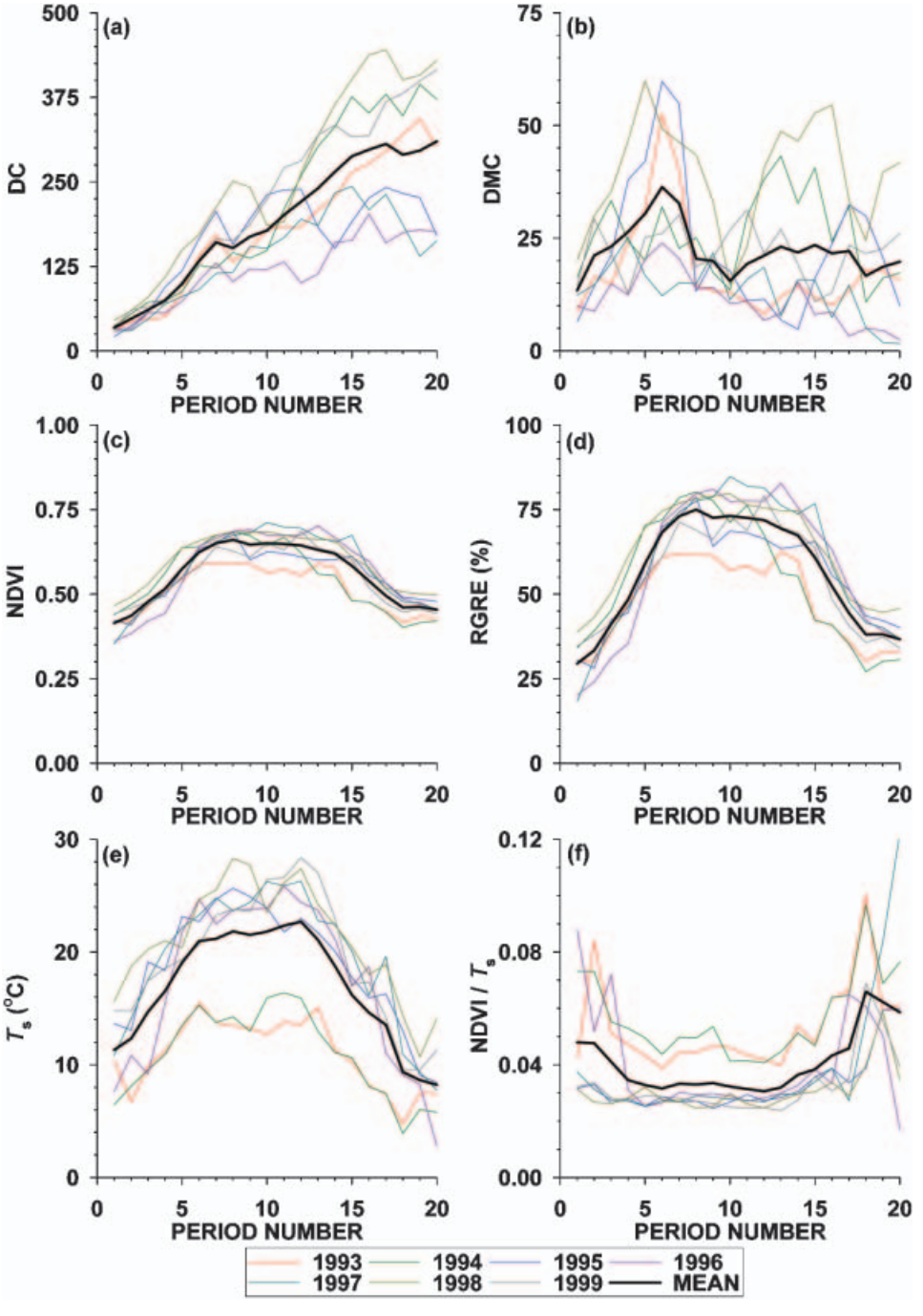

Figure 3. Mean values recorded at all weather stations during the study periods for: (*a*) DC, (*b*) DMC, (*c*) NDVI, (*d*) RGRE, (*e*) T_s, and (*f*) NDVI/T_s. Thin coloured lines represent yearly averages and thick black lines represent study period (1993–1999) averages.

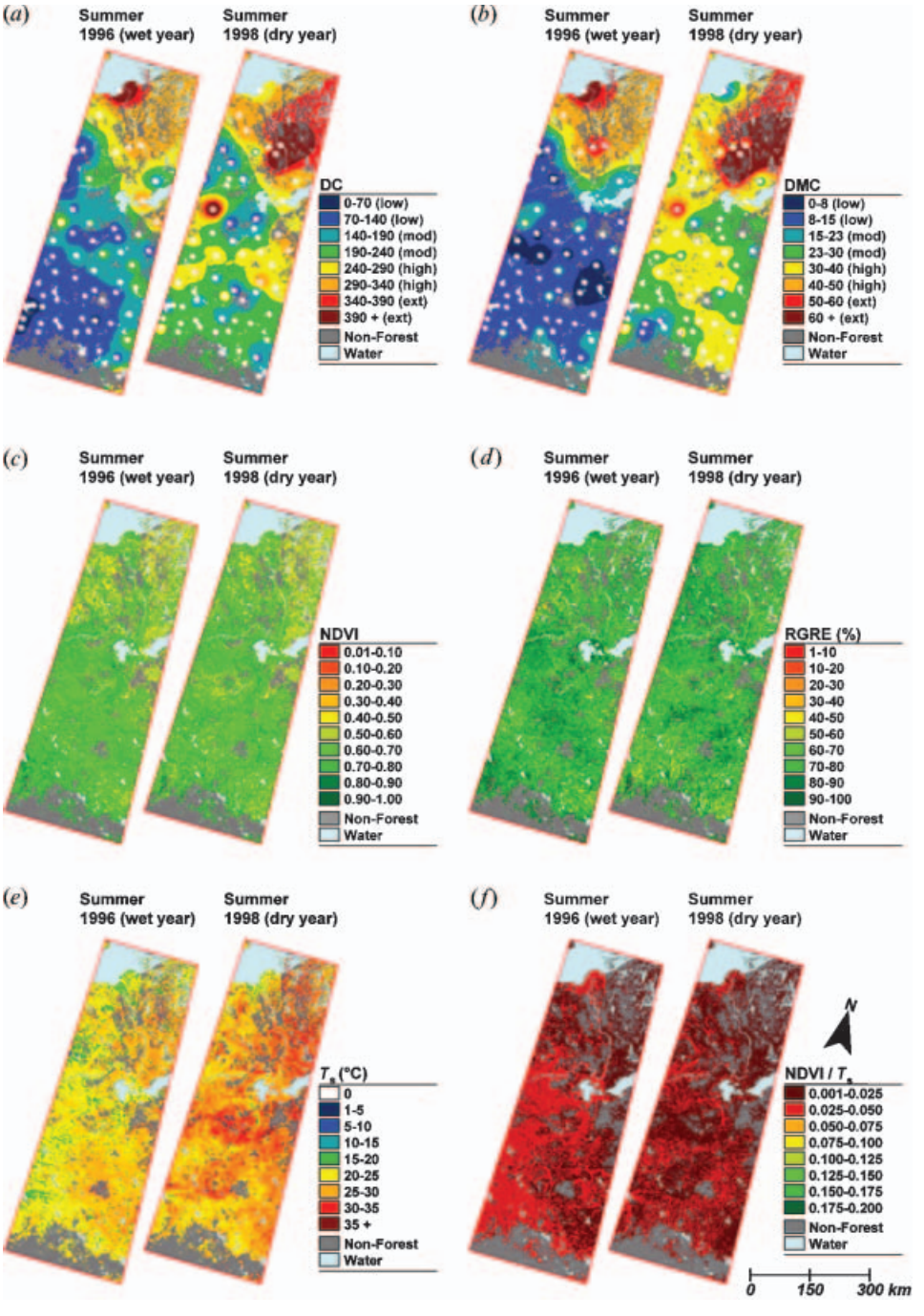

Figure 4. Study area maps of: (*a*) DC, (*b*) DMC, (*c*) NDVI, (*d*) RGRE, (*e*) T_s, and (*f*) NDVI/T_s, showing spatial variability in a wet year (1996) and a dry year (1998) during summer (period 12).

Table 2. *F*-values from an analysis of variance used to assess the relative effects of year, period, broad forest cover type, elevation, and latitude on DC, DMC, NDVI, RGRE, T_s, and NDVI/T_s in NOAA-11 years, and in NOAA-14 years.

Satellite category/factors	Degrees of freedom	*F*-test values for variables tested[1]					
		DC	DMC	NDVI	RGRE	T_s	NDVI/T_s
NOAA-11 years (1993–1994) N=1629, Residual error=0							
Year	1	**22.68**	**7.43**	**53.48**	**25.94**	1.14	0.80
Period	19	**34.70**	**5.83**	**34.21**	**52.40**	**23.92**	**26.67**
Cover[2]	3	**13.18**	**7.24**	**37.59**	**2.73**	2.45	**39.12**
Latitude[3]	3	**4.27**	1.05	1.93	2.02	2.25	**18.43**
Elevation[4]	3	**7.58**	**4.15**	**5.68**	**4.79**	1.87	**19.92**
Year*period	19	**10.97**	**23.04**	**7.14**	**14.30**	**9.70**	**16.67**
Year*cover	3	**5.37**	**2.94**	**5.91**	1.79	0.18	0.73
Year*latitude	3	**3.91**	**13.44**	**4.91**	2.33	0.89	0.54
Year*elevation	3	**25.75**	**8.82**	**3.51**	0.29	**13.47**	**6.95**
Period*cover	52	**1.78**	0.76	**2.47**	**2.02**	**1.35**	**15.62**
Period*latitude	52	1.31	1.11	0.69	1.13	1.22	**21.18**
Period*elevation	53	1.07	0.51	0.65	1.14	0.92	**11.62**
Cover*latitude	5	**3.48**	0.94	**5.74**	2.11	2.20	1.64
Cover*elevation	5	0.50	0.20	**5.70**	**3.26**	1.38	**4.20**
Latitude*elevation	5	**5.24**	**3.49**	**5.61**	0.36	**2.30**	**2.25**
NOAA-14 years (1995–1999) N=4083, Residual error=0							
Year	4	**183.32**	**105.06**	**42.30**	**50.16**	**54.82**	**3.48**
Period	19	**79.57**	**12.22**	**156.30**	**177.55**	**116.30**	**5.50**
Cover[2]	3	**20.43**	**5.28**	**131.17**	**4.72**	**14.21**	**2.36**
Latitude[3]	3	**6.73**	**9.75**	**34.27**	0.17	**4.66**	**6.60**
Elevation[4]	3	**45.55**	**43.97**	**29.82**	**7.37**	**29.73**	**22.43**
Year*period	76	**16.46**	**15.92**	**12.00**	**14.37**	**16.66**	**5.73**
Year*cover	12	**10.75**	**2.99**	**3.97**	**4.32**	1.25	1.08
Year*latitude	12	**14.44**	**9.71**	**4.64**	**5.15**	**3.28**	**3.62**
Year*elevation	12	**4.70**	**4.58**	**1.77**	**2.99**	1.64	**2.39**
Period*cover	57	0.50	**2.50**	**3.60**	**2.39**	**2.21**	**1.37**
Period*latitude	57	**2.19**	**1.85**	**2.40**	**2.64**	**2.46**	**6.57**
Period*elevation	57	**2.38**	**1.95**	**1.42**	**2.33**	1.24	**7.68**
Cover*latitude	4	**3.72**	1.02	**15.36**	**21.02**	**18.59**	**1.62**
Cover*elevation	5	**6.83**	**2.98**	**17.86**	**7.94**	1.90	0.65
Latitude*elevation	5	**6.20**	**22.81**	**17.17**	**9.41**	**4.74**	**2.90**

[1]Plain font (ex. 0.45) not significant, bold font (ex. **0.45**) significant at α=0.05, bold underlined font (ex. **0.45**) significant at α<0.0001.
[2]Cover categories: closed coniferous, closed mixedwood, open coniferous, and open mixedwood.
[3]Latitude categories: 54–55° N, 56–57° N, 58–59° N, and 60–62° N.
[4]Elevation categories: 0–250 m, 251–500 m, 501–750 m, 751–1000 m.

those of closed coniferous, closed mixedwood, and open mixedwood, respectively (Oldford 2004). Closed coniferous and open mixedwood NDVI values were not significantly different. Closed mixedwood NDVI values were significantly greater than closed coniferous and open mixedwood NDVI values in all years except 1996 and 1997 (wet years). The variations in mean NDVI observed between forest cover types were consistent with those found in other studies. In particular, a study of mean NDVI profiles of 12 different land cover types in BOREAS sites with NOAA-AVHRR images collected in 1992 showed that mean NDVI values were greater in

mixed forests than conifer forests (Steyaert *et al.* 1997). Duchemin *et al.* (1999) examined the NDVI recorded from NOAA-AVHRR images between 1988 and 1990 in France, and found that as the pine composition of mixed forests increased, NDVI decreased.

3.2 *DMC and DC modelling*

Modelling DMC and DC from spectral variables was performed for 44 temporal categories. Eleven categories were based on individual years, combined NOAA-11 years (1993–1994), combined NOAA-14 years (1995–1999), wet years (1996–1997), and dry years (1998–1999). Each year was subdivided into four seasonal groups, including the entire season (11 April–31 October), spring (11 April–20 June), summer (21 June–20 September), and fall (21 September–31 October). In each case, regressions were computed for all stations combined and for stations grouped based on elevation, latitude, or broad forest cover type.

The average temperatures observed during spring, summer, and fall periods were 14°C, 18°C, and 7°C, respectively. The warmest year was 1998 (a dry year), with average spring, summer, and fall temperatures of 16°C, 20°C, and 8°C, respectively. The coolest year was 1996 (a wet year), with average spring, summer, and fall temperatures of 13°C, 17°C, and 4°C, respectively. The average total rainfall observed during spring, summer, and fall periods were 87 mm, 193 mm, and 26 mm, respectively. The driest year was 1998, with average total spring, summer, and fall rainfalls of 47 mm, 163 mm, and 21 mm, respectively. The wettest year was 1996, with average spring, summer, and fall rainfalls of 123 mm, 236 mm, and 44 mm, respectively. The apparent low total fall rainfall amounts were due to fewer weather stations collecting data for the entire fall season. In reality, fall is typically wetter than spring or summer in Canada's boreal forests.

Significant correlations were found in 86% of spring cases, 71% of summer cases, 64% of entire year cases, and 18% of fall cases (table 3). Spring Pearson's correlation coefficients for DMC and DC were, respectively, 59% and 73% greater than those of other seasons. Overall, DMC was correlated most often to T_s, and DC to NDVI (table 3). While a number of correlations were significant ($p<0.05$), quite often their Pearson's correlation coefficients were low. This meant that, individually, spectral variables were poor indicators of DMC and DC.

The strongest correlations for both DMC and DC occurred in 1993 and 1995 (two normal rainfall years), and the weakest were in 1998 (a dry year). For DMC, the highest correlation ($r=0.58$) occurred with T_s in the spring of 1993. For DC, the highest correlation ($r=0.68$) occurred with RGRE in the spring of 1995. Previous studies also have found strong correlations between DC and NDVI. Negative r values between NDVI and DC were observed previously by Camia *et al.* (1999) over Mediterranean shrublands and grasslands, by Aguado *et al.* (2003) over Mediterranean forests, and by Dominguez *et al.* (1994) over Canadian boreal forests and grasslands. Positive r values, like those of this study, were observed by Leblon *et al.* (2001) over northern boreal forests for the whole year. Positive relationships between DC and T_s were observed over Mediterranean forests (Aguado *et al.* 2003), but not over Mediterranean shrublands and grasslands (Camia *et al.* 1999) and over Canadian boreal forests and grasslands (Dominguez *et al.* 1994).

Table 3. Pearson's correlation coefficients and stepwise regression model adjusted R^2 values for relationships between spectral variables and slow-drying fuel moisture codes during all season, spring, summer, and fall periods.

			Pearson's correlation coefficients[(1)]								Stepwise regression adj. $R^{2(1)}$	
			DMC				DC					
Season	Year(s)	N	NDVI	RGRE	T_s	NDVI/ T_s	NDVI	RGR-E	T_s	NDVI/ T_s	DMC	DC
All season periods (1 to 20)	1993	816	0.05	**0.16**	**0.34**	**−0.12**	−0.04	**0.14**	**0.08**	0.06	**0.12**	**0.08**
	1994	813	**−0.28**	**−0.11**	**0.16**	**−0.15**	**−0.42**	**−0.36**	**−0.10**	−0.02	**0.16**	**0.18**
	1995	790	−0.04	0.03	**0.16**	**−0.16**	**0.18**	**0.25**	0.06	0.05	**0.03**	**0.07**
	1996	772	**−0.08**	**0.09**	**0.33**	**−0.20**	**−0.07**	**0.15**	0.07	**−0.09**	**0.19**	**0.17**
	1997	756	**−0.10**	−0.03	**0.26**	**−0.12**	**0.15**	**0.24**	**0.17**	−0.06	**0.12**	**0.06**
	1998	843	−0.01	0.01	0.04	−0.06	−0.06	0.02	−0.05	**0.07**	0.00	**0.02**
	1999	922	0.03	0.04	**0.18**	**−0.09**	**0.15**	**0.12**	**0.08**	**0.12**	**0.04**	**0.05**
	Dry	1765	**0.07**	**0.09**	**0.11**	**−0.06**	**0.06**	**0.09**	0.03	**0.09**	**0.01**	**0.02**
	Wet	1528	**−0.09**	0.04	**0.31**	**−0.13**	0.04	**0.20**	**0.13**	**−0.07**	**0.16**	**0.09**
	NOAA-11	1629	**−0.09**	0.05	**0.24**	**−0.13**	**−0.23**	**−0.12**	−0.02	0.02	**0.10**	**0.07**
	NOAA-14	4083	−0.02	0.03	**0.16**	**−0.09**	**0.05**	**0.11**	**0.08**	−0.01	**0.03**	**0.02**
Spring periods (1 to 7)	1993	331	**0.45**	**0.55**	**0.58**	**−0.21**	**0.55**	**0.65**	**0.56**	**−0.14**	**0.46**	**0.53**
	1994	290	**−0.24**	−0.06	**0.24**	**−0.37**	**0.16**	**0.37**	**0.45**	**−0.34**	**0.18**	**0.26**
	1995	287	**0.40**	**0.51**	**0.50**	**−0.12**	**0.65**	**0.68**	**0.46**	0.08	**0.32**	**0.49**
	1996	272	**0.13**	**0.31**	**0.44**	**−0.15**	**0.49**	**0.62**	**0.56**	**−0.15**	**0.27**	**0.45**
	1997	275	**−0.24**	**−0.21**	**0.05**	**−0.28**	**0.43**	**0.51**	**0.46**	−0.01	**0.09**	**0.31**
	1998	313	**0.23**	**0.23**	**0.17**	0.03	**0.51**	**0.56**	**0.50**	0.01	**0.06**	**0.42**
	1999	328	**0.13**	0.08	**0.33**	**−0.15**	**0.47**	**0.42**	**0.51**	−0.07	**0.10**	**0.37**
	Dry	641	**0.31**	**0.28**	**0.29**	−0.01	**0.53**	**0.52**	**0.53**	−0.02	**0.13**	**0.43**
	Wet	547	−0.02	**0.11**	**0.28**	**−0.14**	**0.46**	**0.57**	**0.49**	**−0.10**	**0.13**	**0.37**
	NOAA-11	621	0.03	**0.14**	**0.43**	**−0.32**	**0.33**	**0.45**	**0.51**	**−0.23**	**0.21**	**0.34**
	NOAA-14	1475	**0.23**	**0.26**	**0.27**	**−0.06**	**0.50**	**0.54**	**0.45**	−0.03	**0.09**	**0.35**
Summer periods (8 to 16)	1993	452	**−0.18**	**0.10**	**0.24**	**−0.27**	**−0.41**	**−0.12**	**0.15**	**−0.34**	**0.12**	**0.21**
	1994	475	**−0.39**	**−0.25**	0.07	**−0.32**	**−0.58**	**−0.51**	**−0.11**	**−0.28**	**0.18**	**0.34**
	1995	440	**−0.23**	0.01	**0.17**	**−0.20**	**−0.09**	−0.06	−0.06	0.00	**0.12**	**0.01**
	1996	432	**−0.28**	**0.12**	**0.27**	**−0.31**	**−0.47**	−0.07	**0.16**	**−0.33**	**0.17**	**0.25**
	1997	431	**−0.19**	0.00	**0.26**	**−0.30**	**−0.29**	**−0.13**	**0.16**	**−0.25**	**0.10**	**0.11**
	1998	457	**−0.12**	−0.07	0.00	−0.04	**−0.29**	**−0.21**	**−0.18**	−0.01	**0.01**	**0.13**
	1999	518	−0.02	0.08	**0.26**	**−0.25**	**0.09**	−0.02	0.07	−0.01	**0.08**	**0.03**
	Dry	975	0.00	**0.07**	**0.10**	**−0.08**	**−0.07**	**−0.08**	−0.05	0.00	**0.01**	**0.01**
	Wet	863	**−0.22**	0.07	**0.28**	**−0.31**	**−0.36**	**−0.08**	**0.18**	**−0.30**	**0.12**	**0.15**
	NOAA-11	927	**−0.17**	0.01	**0.17**	**−0.24**	**−0.44**	**−0.29**	0.01	**−0.28**	**0.10**	**0.20**
	NOAA-14	2278	**−0.11**	0.00	**0.21**	**−0.21**	**−0.22**	**−0.17**	**0.09**	**−0.19**	**0.05**	**0.06**

Forward stepwise regressions between slow-drying FWI fuel moisture codes and spectral variables were generally stronger for DC than for DMC, with larger adjusted R^2 values reported in 65% of significant cases (table 3). When all stations were combined and analysed for the entire season, significant relationships with DMC and DC were observed for all annual categories, except for DMC in 1998 (a dry year). While many relationships were significant ($p<0.05$), they explained little

Table 3. (*Continued*.)

			Pearson's correlation coefficients[1]								Stepwise regression adj. $R^{2(1)}$	
			DMC				DC					
Season	Year(s)	N	NDVI	RGRE	T_s	NDVI/ T_s	NDVI	RGR-E	T_s	NDVI/ T_s	DMC	DC
Fall periods (17 to 20)	1993	33	−0.33	−0.18	−0.10	0.05	**−0.46**	−0.19	0.28	−0.12	0.08	**0.19**
	1994	48	0.14	**0.29**	**0.34**	−0.10	**−0.33**	−0.22	0.13	−0.06	**0.16**	**0.09**
	1995	63	0.08	0.03	**0.51**	**−0.45**	−0.08	−0.19	0.14	−0.19	**0.30**	**0.09**
	1996	68	0.14	0.05	0.00	0.10	−0.18	−0.12	−0.15	−0.11		0.02
	1997	50	0.25	0.08	**0.45**	−0.14	**0.29**	**−0.33**	0.14	−0.24	**0.21**	**0.31**
	1998	73	−0.22	−0.13	0.09	−0.12	−0.01	0.05	−0.02	−0.10	0.04	
	1999	76	**0.40**	0.11	0.18	0.02	**0.39**	0.16	0.22	−0.06	**0.16**	**0.14**
	Dry	149	−0.02	−0.03	0.14	−0.10	**0.18**	0.13	0.10	−0.09	0.01	**0.02**
	Wet	118	0.15	0.04	**0.38**	−0.10	0.05	**−0.24**	0.06	**−0.20**	**0.13**	**0.10**
	NOAA-11	81	0.03	0.14	0.20	−0.08	**−0.39**	**−0.26**	0.14	−0.10	0.03	**0.15**
	NOAA-14	330	0.00	−0.02	**0.24**	−0.08	0.03	−0.05	**0.23**	**−0.14**	**0.06**	**0.06**

[1]Plain font (ex. 0.45) not significant, bold font (ex. **0.45**) significant at $\alpha=0.05$, bold underlined font (ex. **0.45**) significant at $\alpha<0.0001$.

variation, with an adjusted R^2 range of 0.01–0.19 for DMC and 0.02–0.18 for DC (table 3).

In most cases, relationships with all stations combined improved when the analysis considered seasonal periods separately. The greatest improvement occurred in spring, when all models were significant ($p<0.0001$) and adjusted R^2 ranged from 0.06–0.46 for DMC and 0.26–0.53 for DC. In summer, all models were significant ($p<0.05$) and adjusted R^2 ranged from 0.01–0.18 for DMC and 0.01–0.34 for DC. In fall, significant DMC models existed in 1994, 1995, 1997, and 1999, as well as for wet years and NOAA-14 years, and significant DC models existed in all years, except 1996 and 1998. Adjusted R^2 in fall cases ranged from 0.06–0.30 for DMC and 0.02–0.31 for DC. RMSE of DMC models ranged from 10.24–25.62 for the entire season, 8.56–24.74 for spring, 8.61–31.07 for summer, and 6.56–28.34 for fall. RMSE of DC models ranged from 83.83–138.39 for the entire season, 34.34–57.17 for spring, 81.10–115.70 for summer, and 75.77–154.20 for fall (Oldford 2004). For both DMC and DC models and all four seasonal categories, the lowest RMSE were observed in wet years (1996, 1997) and all the years combined, and the highest RMSE were in 1998 (a dry year) (Oldford 2004). Because the majority of models tested performed better in the spring, further regression analyses considering the effects of spatial factors (elevation, latitude, and broad forest cover type) were performed on this season only.

3.3 *Spring period DMC and DC modelling*

Stepwise multiple regression models predicted DMC and DC in spring reasonably well from NOAA-AVHRR spectral variables, with all models being significant and with quite high adjusted R^2 values (table 4). The spectral variables most often used in stepwise regression spring models for all stations in different yearly categories were RGRE and T_s (Oldford 2004). During spring, both spectral variables and the slow-drying fuel moisture codes increased, but for different reasons. DC, DMC, and

Table 4. Results of stepwise regression models of DMC and DC during spring periods, as a function of year(s), broad forest cover, station latitude, and elevation. Number of observations (N), root mean squared errors (RMSE), and adjusted $R^{2(1)}$ are presented.

				Broad forest cover[(2)]												Latitude						Elevation											
	All stations			cc			cm			oc			om			54–57			58–62			0–250			251–500			501–750			751–1000		
Year(s)	N	RMSE	R^2	N	RMSE	R^2	N	RMSE	R^2	N	RMSE	R^2	N	RMSE	R^2	N	RMSE	R^2	N	RMSE	R^2	N	RMSE	R^2	N	RMSE	R^2	N	RMSE	R^2	N	RMSE	R^2
Duff moisture code																																	
1993	330	13.9	**0.46**	35	8.6	**0.60**	59	10.3	**0.66**	169	15.8	**0.40**	64	12.9	**0.49**	265	12.8	**0.50**	64	17.1	**0.40**	41	17.7	**0.42**	59	13.3	**0.28**	163	13.8	**0.52**	64	9.0	**0.64**
1994	289	16.0	**0.18**	31	8.8	**0.26**	57	18.7	**0.16**	141	18.2	**0.07**	57	10.8	**0.21**	234	13.2	**0.18**	54	18.1	**0.37**	32	16.3	**0.54**	54	17.1	**0.25**	142	11.2	**0.20**	58	10.1	**0.18**
1995	286	20.0	**0.32**	38	19.5	**0.31**	65	17.5	**0.40**	136	22.2	**0.24**	44	16.7	**0.52**	214	20.1	**0.28**	71	19.5	**0.46**	36	18.7	**0.57**	61	20.5	**0.41**	130	20.3	**0.27**	56	15.4	**0.27**
1996	271	10.9	**0.27**	28	6.7	**0.20**	50	6.0		150	13.3	**0.22**	40	7.2	**0.23**	203	7.0	**0.27**	67	15.8	**0.22**	31	11.9	**0.31**	62	14. 7	**0.27**	122	5.9	**0.17**	53	7.5	**0.19**
1997	274	8.6	**0.09**	31	4.4	**0.63**	63	7.3	**0.26**	142	9.3	**0.04**	35	8.2	**0.16**	210	8.4	**0.09**	63	9.0	**0.11**	30	8.3		64	10.6	**0.06**	118	6.5	**0.18**	59	5.0	**0.28**
1998	312	24.7	**0.06**	48	25.9	0.05	61	23.4	**0.09**	159	25.3	**0.09**	41	20.1		224	22.2	**0.04**	87	29.4	**0.15**	36	26. 6	**0.17**	71	27.5	**0.07**	132	25.0	**0.05**	70	16.7	**0.13**
1999	327	12.3	**0.10**	42	10.1	**0.27**	64	13.9	**0.07**	177	11.9	**0.18**	41	7.1	**0.33**	243	12.5	**0.13**	83	11.6	**0.08**	35	11.1	0.08	81	13.3	**0.19**	141	13.0	**0.03**	67	6.5	**0.24**
Wet	640	21.3	**0.13**	91	20.5	**0.15**	126	21.9	**0.09**	337	21.7	**0.15**	83	17.4	**0.22**	468	19.7	**0.15**	171	24.6	**0.15**	72	22.6	**0.16**	153	22.9	**0.13**	274	21.7	**0.13**	138	14.6	**0.27**
Dry	546	10.3	**0.13**	60	5.5	**0.43**	114	7.7	**0.10**	293	12.1	**0.11**	76	8.3	**0.05**	414	8.1	**0.11**	131	14.3	**0.13**	62	11.7	**0.14**	127	13.3	**0.15**	241	6.7	**0.05**	113	6.7	**0.12**
NOAA-11	620	16.6	**0.21**	67	10.6	**0.30**	117	16.7	**0.27**	311	18.0	**0.17**	122	15.2	**0.14**	500	15.6	**0.18**	119	17.9	**0.38**	74	18.0	**0.45**	114	16.8	**0.10**	306	16.5	**0.18**	123	12.0	**0.28**
NOAA-14	1474	20.9	**0.09**	191	20.2	**0.11**	307	21.3	**0.06**	768	21.3	**0.10**	205	19.2	**0.13**	1098	20.0	**0.08**	375	22.8	**0.13**	172	21.3	**0.18**	343	22.0	**0.11**	647	21.3	**0.07**	309	15.6	**0.12**
Drought code																																	
1993	330	39.4	**0.53**	35	35.9	**0.48**	59	39.7	**0.56**	169	40.7	**0.51**	64	32.1	**0.70**	265	36.8	**0.59**	64	48.7	**0.32**	41	52.8	**0.32**	59	36.3	**0.55**	163	37.6	**0.60**	64	33.5	**0.56**
1994	289	44.9	**0.26**	31	33.5	**0.38**	57	45.3	**0.30**	141	49.4	**0.24**	57	31.8	**0.25**	234	40.2	**0.27**	54	49.1	**0.45**	32	50.5	**0.53**	54	50.9	**0.30**	142	34.5	**0.25**	58	36.6	**0.13**
1995	286	51.9	**0.49**	38	41.0	**0.65**	65	42.3	**0.71**	136	56.9	**0.34**	44	38.3	**0.75**	214	50.9	**0.52**	71	51.7	**0.46**	36	49.5	**0.55**	61	50.3	**0.55**	130	54.7	**0.49**	56	36.9	**0.65**
1996	271	34.3	**0.45**	28	26.1	**0.51**	50	32.3	**0.31**	150	35.8	**0.49**	40	25.7	**0.58**	203	30.3	**0.46**	67	44.8	**0.36**	31	41.9	**0.43**	62	33.5	**0.66**	122	29.8	**0.38**	53	23.7	**0.41**
1997	274	34.5	**0.31**	31	27.4	**0.55**	63	31.5	**0.28**	142	36.0	**0.32**	35	33.6	**0.36**	210	30.6	**0.36**	63	43.7	**0.26**	30	39.4	**0.48**	64	28.8	**0.64**	118	26.7	**0.31**	59	23.7	**0.35**
1998	312	57.2	**0.42**	48	45.9	**0.54**	61	50.8	**0.52**	159	61.2	**0.40**	41	45.8	**0.56**	224	55.7	**0.41**	87	61.4	**0.43**	36	63.0	**0.47**	71	54.1	**0.56**	132	55.3	**0.41**	70	48.3	**0.48**
1999	327	47.5	**0.37**	42	38.3	**0.40**	64	49.0	**0.35**	177	46.9	**0.42**	41	38.9	**0.57**	243	48.4	**0.39**	83	41.3	**0.38**	35	39.0	**0.51**	81	47.5	**0.47**	141	52.6	**0.30**	67	30.3	**0.53**
Wet	640	52.7	**0.43**	91	43.3	**0.49**	126	51.2	**0.44**	337	54.2	**0.44**	83	43.5	**0.57**	468	52.3	**0.42**	171	53.4	**0.44**	72	53.1	**0.50**	153	51.3	**0.54**	274	54.0	**0.39**	138	42.5	**0.48**
Dry	546	34.9	**0.37**	60	27.6	**0.50**	114	32.0	**0.29**	293	36.7	**0.40**	76	30.1	**0.45**	414	30.8	**0.40**	131	43.8	**0.34**	62	39.9	**0.47**	127	32.5	**0.62**	241	28.9	**0.32**	113	24.6	**0.35**

Table 4. (*Continued*.)

				Broad forest cover[2]												Latitude						Elevation											
	All stations			cc			cm			oc			om			54–57			58–62			0–250			251–500			501–750			751–1000		
Year(s)	*N*	RMSE	R^2	*N*	RMSE	R^2	*N*	RMSE	R^2	*N*	RMSE	R^2	*N*	RMSE	R^2	*N*	RMSE	R^2	*N*	RMSE	R^2	*N*	RMSE	R^2	*N*	RMSE	R^2	*N*	RMSE	R^2	*N*	RMSE	R^2
NOAA-11	620	44.6	**0.34**	67	40.2	**0.24**	117	45.3	**0.37**	311	47.0	**0.33**	122	38.0	**0.41**	500	42.7	**0.34**	119	50.6	**0.35**	74	54.5	**0.38**	114	47.3	**0.33**	306	40.3	**0.39**	123	41.2	**0.20**
NOAA-14	1474	52.5	**0.35**	191	45.8	**0.42**	307	54.0	**0.36**	768	53.0	**0.34**	205	48.8	**0.44**	1098	52.7	**0.33**	375	52.0	**0.38**	172	48.9	**0.49**	343	49.6	**0.48**	647	55.2	**0.29**	309	43.5	**0.37**

[1]Plain font (ex. 0.45): not significant, bold font (ex. **0.45**): significant at $\alpha=0.05$, bold underlined font (ex. **0.45**): significant at $\alpha<0.0001$, blank cells: no variables met the $\alpha \leqslant 0.15$ requirement for entry into the stepwise regression model.
[2]cc: closed coniferous, cm: closed mixedwood, oc: open coniferous, and om: open mixedwood.

T_s increased because of low precipitation and increasing air temperatures, while NDVI and RGRE increased because of vegetation green-up. Leblon *et al.* (2001) reached a similar conclusion regarding high correlation between DC or DMC and cumulative NDVI data from northern boreal forests.

Good spring model performance was consistent with results over Mediterranean forests of southern Spain. Aguado *et al.* (2003) found spectral models predicted DC better in later summer and fall, the driest seasons in Mediterranean climates. Under boreal conditions (particularly in Western Canada), the driest season is spring, when there is less rainfall and often little melting snow to saturate soils. Also, frost and frozen soil in early spring may make soil water unavailable.

DMC models were the best during two normal rainfall years, 1993 (adjusted R^2=0.46) and 1995 (adjusted R^2=0.32). In all years, DC models produced better results than DMC models, with adjusted R^2 values between 0.26 and 0.53.

When weather station locations were categorized by broad forest cover type, DMC and DC model variability were best explained in closed coniferous and open mixedwood types with higher adjusted R^2 values more often than those of closed mixedwood and open coniferous types (table 4). RMSE of DMC and DC models were lower for closed coniferous and open mixedwood types more often than those of closed mixedwood and open coniferous types. When weather station locations were categorized by latitude, compared with all station locations combined, DMC and DC models had higher adjusted R^2 values for both low and high latitude locations at different temporal periods (table 4). RMSE of DMC and DC models for low latitude station locations were slightly lower than those of high latitude station locations in most years, except in 1995 and 1999 for DMC and 1999 and NOAA-14 years for DC. When weather station locations were categorized by elevation, DMC and DC model variability were best explained in 0–250 m, 251–500 m, and 751–1000 m categories with higher adjusted R^2 values more often than those of the 501–750 m category (table 4). RMSE of DMC and DC models were lower for the 751–1000 m category more often than other elevation categories.

One of the greatest model improvements resulting from categorizing weather station locations spatially was for DC in the spring of 1995, for stations grouped by broad forest cover types. In this case, non-spatially categorized adjusted R^2 was 0.49. Adjusted R^2 values were higher for closed coniferous stations (0.65), for closed mixedwood stations (0.71), and for open mixedwood stations (0.75), but were lower for open coniferous stations (0.34) (table 4). The reduced adjusted R^2 for open coniferous cover types may have resulted from this cover type being composed of a mixture of shrub, moss, lichen, and soil under-storeys. For this land cover class, DC models saturated at observed DC values somewhere between 125 and 175, which corresponds to the DC threshold values of 140 between low and moderate danger rating (figure 5). The saturation observed in DC models likely resulted from the inclusion of NDVI or RGRE as model independent variables. These spectral variables have a maximum value (as shown in Oldford 2004), while DC did not have a maximum value limit.

3.4 *DC mapping*

For demonstration purposes, the four DC models (closed and open coniferous and mixedwood) developed for 1995 (figure 5) were used to map DC in period 6 (1–10 June 1995) for a 15 × 15 pixel area located in the south of the study area surrounding a fire that started on 2 June 1995 and burned 162 ha in the next 16 days (figure 6).

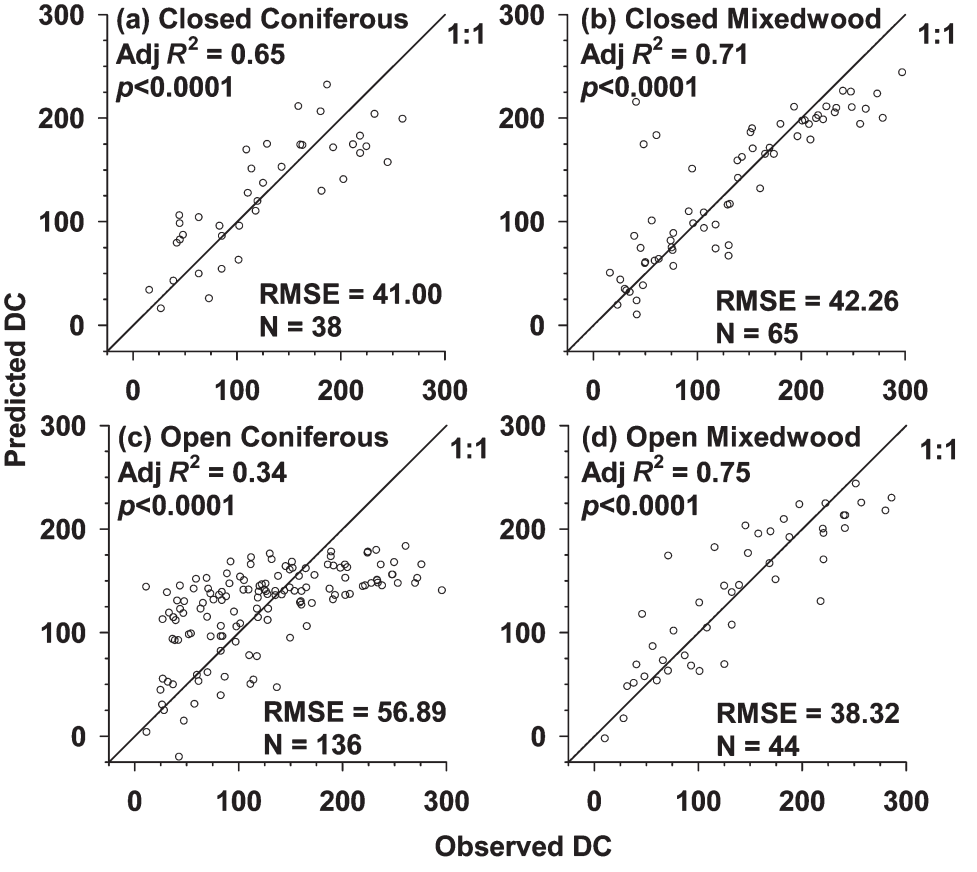

Figure 5. Plots of observed vs. predicted DC characterized by four broad forest cover types in spring 1995. Predictions were made with the following models: (*a*) DC = −434.52 + 1041.13 NDVI − 2.68 RGRE + 3.70 T_s; (*b*) $DC = -57.36 + 2.79$ RGRE + 2.51 T_s; (*c*) DC = −24.88 + 2.52 RGRE; (*d*) DC = 40.37 + 3.59 RGRE − 3028.04 NDVI/T_s. Solid lines represent a 1:1 relationship.

The 15 × 15 pixel area was almost completely composed of tree-dominated cover with open coniferous, closed coniferous, closed mixedwood, and open mixedwood making up 56%, 20%, 15%, and 7% of the area, respectively. The fire shown in the centre of the 15 × 15 pixel area was classified by the Sustainable Resource Development Department of Alberta as a surface fire, caused by lightning. Two weather stations were located between 30 km and 35 km south and north of the fire. Comparisons between the spectrally derived maps and weather station interpolated DC maps showed how improved spatial resolution can be achieved at the pixel level using remote sensing images compared with weather station interpolation. The region that burned from 2–17 June 1995 was located in a closed coniferous cover type to the south, and an open coniferous cover type to the north. It was interesting to observe that the fire burned in a closed coniferous forest cover type that was classified as having a high DC danger rating when the NOAA-AVHRR image was used, but it was classified as having a moderate DC danger rating in the weather station-based map. In this case, remote sensing has the potential to be more useful than the weather station-based map in predicting drought conditions in relationship

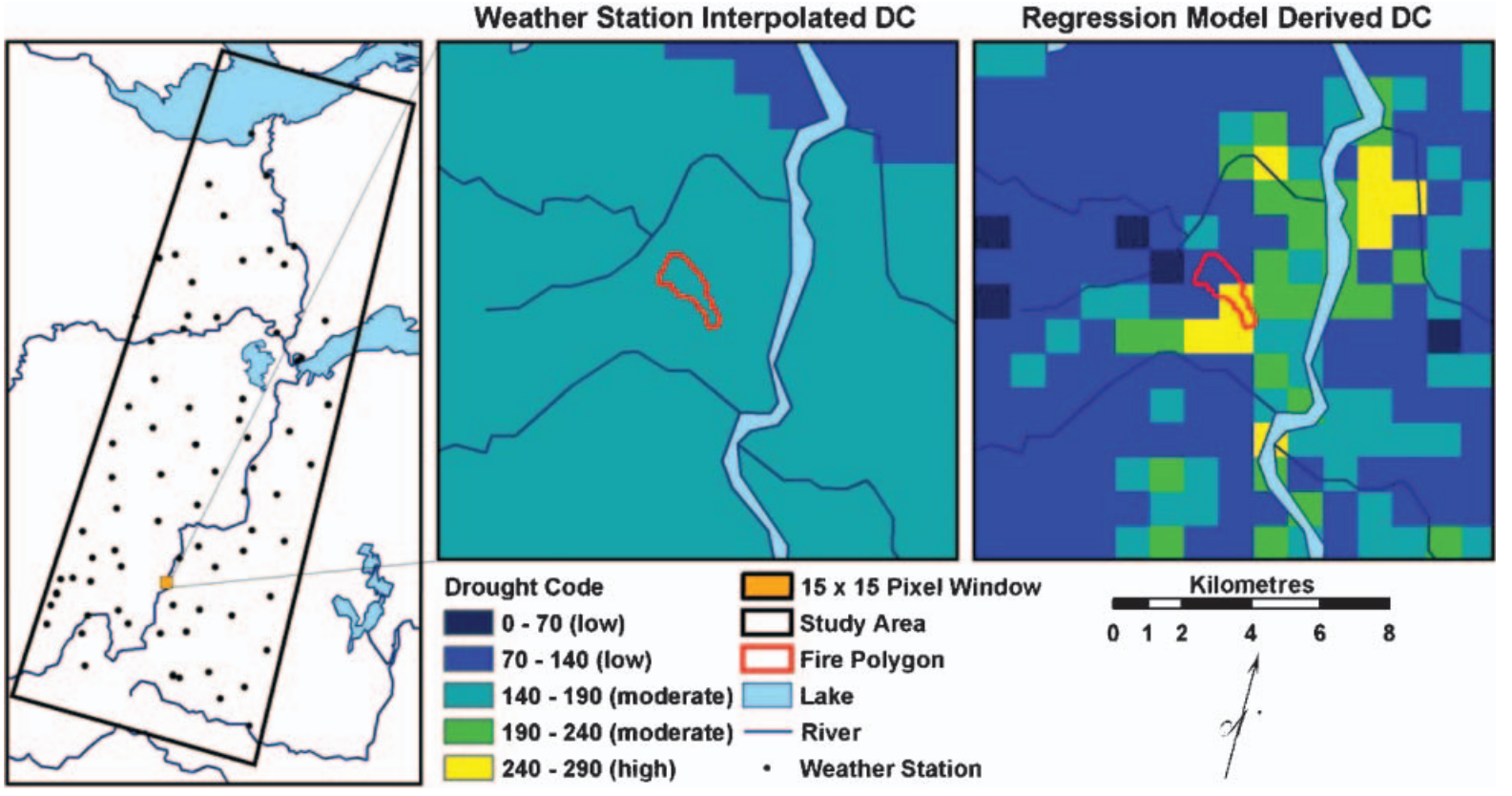

Figure 6. Comparison between DC mapped by weather station interpolation and stepwise multiple regression models for period 6 (1–10 June), 1995. The fire polygon corresponds to a 162 ha area burned between 2–17 June 1995.

to fire occurrence. However, the regions having an open coniferous cover type corresponded to a low DC danger rating on the spectrally derived map, compared to a moderate DC danger rating on the weather station-based map. This was expected because spectrally derived DC models for open coniferous cover types explained only 34% of the variation and underestimated DC values beyond about 140 (low danger category).

4. Conclusions

The objective of this study was to determine if NOAA-AVHRR optical and thermal-infrared remote sensing images were related to slow-drying fuel moisture conditions, as parameterized by DMC and DC of the FWI system. In doing so, it was found that temporal (year and season) and spatial factors (broad forest cover types, elevations, latitudes) had a great influence on DMC, DC, NDVI, RGRE, T_s, and NDVI/T_s. Because of the influence of these factors, data were grouped into temporal and spatial categories for modelling purposes. By combining spectral variables through linear stepwise multiple regression, DC predictions were stronger than DMC predictions. Better results were observed under spring conditions than in summer, fall, or the entire year.

Single 10-day composite NOAA-AVHRR optical and thermal-infrared images could predict slow-changing fuel moisture conditions under spring conditions in certain years, with the best results being observed in closed coniferous and closed and open mixedwood areas. These images were poor predictors of DMC and DC for other seasons, probably because they do not consider previous period effects on the spectral response of the forest. Further studies are needed to test if results could be improved using multi-period NOAA-AVHRR images, such as in Dominguez *et al.* (1994) and Leblon *et al.* (2001). While promising results were observed in some cases, it was not possible to establish a single generalized model to predict slow-drying fuel moisture codes with NOAA-AVHRR images under all conditions.

NOAA-AVHRR images with a 1 km spatial resolution might be too coarse for approximating the diverse conditions found in Canada's boreal forest. Remotely sensed images with improved spatial resolutions, like those provided by the MODIS sensor, with a spatial resolution of 250 m should be tested. However, like AVHRR, MODIS images cannot be acquired during cloudy conditions. Such a limitation is overcome with SAR images like those provided by ERS-1, ENVISAT, and RADARSAT. ERS-1 and RADARSAT-1 SAR images have been related to FWI codes and indices (Bourgeau-Chavez *et al.* 1999, Abbott *et al.* 2002, Leblon *et al.* 2002), but these studies occurred in homogeneous stands. Further work is needed to assess the potential use of SAR images in estimating FWI codes and indices in large and diverse areas, like the one of this study.

This research is necessary because new research shows that boreal forest fires are increasing in number, area, and occurrence, which may be linked to global climate change. With an improved understanding of the relationship between remotely sensed spectral data and fuel moisture conditions, fire danger prediction can be improved.

Acknowledgements

This study was funded by the National Science and Engineering Research Council of Canada and the Canadian Forest Service. Satellite imagery was provided by Rob Fraser and Rasim Latifovic of the Canada Center for Remote Sensing. Weather

data were provided by the Canadian Forest Service, Alberta Department of Energy and Environment, Northwest Territories Forest Management Division, and Parks Canada. We are thankful to Meg Krawchuk for her help in acquiring weather data. We express our appreciation to Dr Rolf Turner of the University of New Brunswick Statistics Department and Dr John Kershaw and Hannelie Botha of the University of New Brunswick Faculty of Forestry for their assistance in statistics and analysis during this study.

References

Abbott, K., Leblon, B., Staples, G., Alexander, M.E. and Maclean, D., 2002, Use of RADARSAT-1 images to map forest fuel moisture over boreal forests. In *Proceedings of the IEEE International Geoscience and Remote Sensing Symposium and 24th Canadian Symposium on Remote Sensing*, June 2002, Toronto, Ontario, pp. 134–136.

Aguado, I., Chuvieco, E., Martin, P. and Salas, J., 2003, Assessment of forest fire danger conditions in southern Spain from NOAA images and meteorological indexes. *International Journal of Remote Sensing*, **24**, pp. 1653–1668.

Bourgeau-Chavez, L.L., Kasischke, E.S. and Rutherford, M.D., 1999, Evaluation of ERS SAR data for prediction of fire danger in a boreal region. *International Journal of Wildland Fire*, **9**, pp. 183–194.

Burgan, R.E., Hartford, R.A. and Eidenshink, J.C., 1996, *Using NDVI to Assess Departure from Average Greenness and its Relation to Fire Business*, General Technical Report, INT-GTR-333, United States Department of Agriculture, Forest Service, Intermountain Research Station, Ogden, Utah, USA.

Burgan, R.E., Klaver, R.W. and Klaver, J.M., 1998, Fuel models and fire potential from satellite and surface observations. *International Journal of Wildland Fire*, **8**, pp. 159–170.

Camia, A., Bovio, G., Aguado, I. and Stach, N., 1999, Meteorological fire danger indices and remote sensing. In *Remote Sensing of Large Wildfires in the European Mediterranean Basin*, E. Chuvieco (Ed), pp. 33–59 (Berlin: Springer-Verlag).

Camia, A., Leblon, B., Cruz, M., Carlson, J. and Aguado, I., 2003, Methods used to estimate moisture content of dead wildland fuels. In *Wildland Fire Danger Estimation and Mapping. The Role of Remote Sensing Data*, pp. 91–117 (London: World Scientific).

Canada Center for Remote Sensing, 2000, ABC3 Canada-wide 1 km AVHRR composite maps (version 2). Special Publication, NBIOME Project, Canada Center for Remote Sensing, Ottawa, Ontario, Canada.

Canadian Council of Forest Ministers, 2004, National Forestry Database Program. Available online at: http://nfdp.ccfm.org (accessed 23 August 2004).

Chuvieco, E., Deshayes, M., Stach, N., Cocero, D. and Riano, D., 1999, Short-term fire risk: foliage moisture content estimation from satellite data. In *Remote Sensing of Large Wildfires in the European Mediterranean Basin*, E. Chuvieco (Ed), pp. 17–38 (Berlin: Springer-Verlag).

Cihlar, J., 1996, Identification of contaminated pixels in AVHRR composite images for studies of land biosphere. *Remote Sensing of Environment*, **56**, pp. 149–163.

Cihlar, J., Chen, J. and Li, Z., 1997a, Seasonal AVHRR multichannel datasets and products for studies of surface–atmosphere interactions. *Journal of Geophysical Research*, **102**, pp. 29625–29640.

Cihlar, J., Ly, H., Li, Z., Chen, J., Pokrant, H. and Huang, F., 1997b, Multitemporal, multichannel AVHRR datasets for land biosphere studies – artifacts and correlations. *Remote Sensing of Environment*, **60**, pp. 35–57.

Cihlar, J., Beaubien, J. and Latifovic, R., 2002, *Land Cover of Canada 1998*, Special Publication, NBIOME Project, Canada Center for Remote Sensing and Natural Resources Canada, Canadian Forest Service, Ottawa, Ontario, Canada.

DESBOIS, N. and VIDAL, A., 1995, La télédétection dans la prévision des incendies de forêt. *Ingénieries-EAT*, **1**, pp. 21–29.

DOMINGUEZ, L., LEE, B.S., CHUVIECO, E. and CIHLAR, J., 1994, Fire danger estimation using AVHRR images in the prairie provinces of Canada. In *Proceedings of the 2nd International Conference of Forest Fire Research*, November 1994, Coimbra, Portugal, **2**, pp. 679–690.

DUCHEMIN, B., GUYON, D. and LAGOUARDE, J., 1999, Potential and limits of NOAA-AVHRR temporal composite data for phenology and water stress monitoring of temperate forest ecosystems. *International Journal of Remote Sensing*, **20**, pp. 895–917.

EIDENSHINK, J.C., HASS, R.H., ZOKAITES, D.M., OHLEN, D.O. and GALLO, K.P., 1989, Integration of remote sensing and GIS technology to monitor fire danger in the northern Great Plains. In *Proceedings of the National GIS Conference*, Ottawa, Ontario, pp. 944–956.

FLOHN, H., 1969, *General Climatology 2*, 266 p (Amsterdam: Elsevier).

GEOGRATIS CANADA, 2000, Digital elevation map of Canada. Available online at: http://geogratis.cgdi.gc.ca/download/gtopo30/canada_dem.zip (accessed 19 January 2004).

GUINDON, B., GOODENOUGH, D.G. and TEILLET, P.M., 1982, The role of digital terrain models in the remote sensing of forests. *Canadian Journal of Remote Sensing*, **8**, pp. 4–16.

ILLERA, P., FERNANDEZ, A. and DELGADO, J.A., 1996, Temporal evolution of the NDVI as an indicator of forest fire danger. *International Journal of Remote Sensing*, **17**, pp. 1093–1105.

HOLBEN, B.N., 1986, Characteristics of maximum value composite images from temporal AVHRR data. *International Journal of Remote Sensing*, **7**, pp. 1417–1434.

LAWSON, B.D., DALRYMPLE, G.N. and HAWKES, B.C., 1997, *Predicting Forest Floor Moisture Content from Duff Moisture Code Values*, Technology Transfer Notes 6, Natural Resources Canada, Canadian Forest Service, Pacific Forestry Center, Vancouver, British Columbia, Canada.

LEBLON, B., 2001, Forest wildfire hazard monitoring using remote sensing: a review. *Remote Sensing Reviews*, **20**, pp. 1–43.

LEBLON, B., 2005, Using remote sensing for fire danger monitoring. *Natural Hazards*, **35**, pp. 343–359.

LEBLON, B., ALEXANDER, M., CHEN, J. and WHITE, S., 2001, Monitoring fire danger of northern boreal forests with NOAA-AVHRR NDVI images. *International Journal of Remote Sensing*, **22**, pp. 2839–2846.

LEBLON, B., KASISCHKE, E., ALEXANDER, M., DOYLE, M. and ABBOTT, M., 2002, Fire danger monitoring using ERS-1 SAR images in the case of northern boreal forests. *Natural Hazards*, **27**, pp. 231–255.

LOPEZ, S., GONZALEZ, F., LLOP, R. and CUEVAS, J.M., 1991, An evaluation of the utility of NOAA-AVHRR images for monitoring forest fire risk in Spain. *International Journal of Remote Sensing*, **12**, pp. 1841–1851.

OLDFORD, S., 2004, Predicting slow-drying fire weather index fuel moisture codes with NOAA-AVHRR images in Canada's northern boreal forests. MSc thesis, Faculty of Forestry and Environmental Management, University of New Brunswick, Fredericton, New Brunswick, pp. 140.

OLDFORD, S., LEBLON, B., GALLANT, L. and ALEXANDER, M., 2003, Mapping pre-fire forest conditions with NOAA-AVHRR images in northern boreal forests. *Geocarto International*, **18**, pp. 21–32.

PALTRIDGE, G.W. and BARBER, J., 1988, Monitoring grassland dryness and fire potential in Australia with NOAA-AVHRR data. *Remote Sensing of Environment*, **25**, pp. 381–394.

PIERCE, L.L., RUNNING, S.W. and GEORGE, A.R., 1990, Remote detection of canopy water stress in coniferous forests using the NS001 thematic mapper simulator and the

thermal infrared multispectral scanner. *Photogrammetric Engineering and Remote Sensing*, **56**, pp. 579–586.

ROWE, J.S., 1972, *Forest Regions of Canada*, Publication no. 1300, Natural Resources Canada, Canadian Forest Service, Ottawa, Ontario, Canada.

SAS INSTITUTE INC., 2001, *The SAS System for Windows, Version 8.02*, SAS Institute Inc., Cary, NC, USA.

STEYAERT, L., HALL, F. and LOVELAND, T., 1997, Land cover mapping, fire regeneration, and scaling studies in the Canadian boreal forest with 1 km AVHRR and Landsat TM data. *Journal of Geophysical Research*, **102**, pp. 29581–29598.

STOCKS, B.J., LAWSON, B.D., ALEXANDER, M.E., VAN WAGNER, C.E., MCALPINE, R.S., LYNHAM, T.J. and DUBE, D.E., 1989, The Canadian forest fire danger rating system: an overview. *The Forestry Chronicle*, **65**, pp. 450–457.

TEILLET, P.M., GUINDON, B. and GOODENOUGH, D.G., 1982, On the slope aspect correction of multi-spectral scanner data. *Canadian Journal of Remote Sensing*, **8**, pp. 84–106.

VAN WAGNER, C.E., 1987, *Development and Structure of the Canadian Forest Fire Weather Index*, Forestry Technical Report 35, Government of Canada, Canadian Forestry Service, Petawawa National Forestry Institute, Ottawa, Ontario, Canada.